

Behavior of piled rafts overlying a tunnel in sandy soil

Raid R. Al-Omari^{1a}, Adel A. Al-Azzawi^{*1} and Kadhim A. AlAbbas^{2b}

¹ Civil Engineering Department, Nahrain University, Baghdad, Iraq

² Civil Engineering Department, Al-Qadisia University, Al-Qadisia, Iraq

(Received December 12, 2014, Revised January 23, 2016, Accepted February 06, 2016)

Abstract. The present research presents experimental and finite element studies to investigate the behavior of piled raft-tunnel system in a sandy soil. In the experimental work, a small scale model was tested in a sand box with load applied vertically to the raft through a hydraulic jack. Five configurations of piles were tested in the laboratory. The effects of pile length (L), number of piles in the group and the clearance distance between pile tip and top of tunnel surface (H) on the load carrying capacity of the piled raft-tunnel system are investigated. The load sharing percent between piles and rafts are included in the load-settlement presentation. The experimental work on piled raft-tunnel system yielded that all piles in the group carry the same fraction of load. The load carrying capacity of the piled raft-tunnel model was increased with increasing (L) for variable (H) distances and decreased with increasing (H) for constant pile lengths. The total load carrying capacity of the piled raft-tunnel model decreases with decreasing number of piles in the group. The total load carrying capacity of the piles relative to the total applied load (piles share) increases with increasing (L) and the number of piles in the group. The increase in (L/H) ratio for variable (H) distance and number of piles leads to an increase in piles share. ANSYS finite element program is used to model and analyze the piled raft-tunnel system. A three dimensional analysis with elastoplastic soil model is carried out. The obtained results revealed that the finite element method and the experimental modeling are rationally agreed.

Keywords: piled raft; tunnel; load test; piles share; finite element

1. Introduction

In recent years, there has been an increasing recognition of the use of piles to reduce raft settlements that can lead to a considerable economy without compromising the safety and performance of the foundation. Such a foundation makes use of both raft and piles, and is referred to as piled raft. In piled raft foundation the raft and piles both contribute in load sharing. The raft carries load through contact with soil while piles carry load through skin friction and end bearing. The piled raft is a more economical foundation compared to pile foundation and undergoes less settlement than that of the raft foundation. The construction and operation of tunnel systems beneath foundations can cause soil movement due to the stress released by tunneling which inevitably causes ground movement around a tunnel. If these movements become excessive, they can damage adjacent buildings and overlaying facilities. The prediction of surface and subsurface

*Corresponding author, Assistant Professor, E-mail: dr_adel_azzawi@yahoo.com

^a Professor

^b Lecturer

settlement trough and the assessment of tunnel stability are very important for the designer's task for ensuring safe construction and appropriate protective measures for buildings situated near a tunnel project.

Benton and Phillips (1991) studied the behavior of two existing tunnels (British Telecom shallow tunnel and deep tunnel) during the construction and loading of large diameter bored piles, supporting new high-rising buildings in London. A two dimensional finite element program called SAFE was used to analyze linearly the interaction of the pair of piles. It was found that the shallow tunnel would displace away from the piles by 3 mm due to loading of the piles. Also, It was noted that relatively simple 2D FE programs are not suitable to analyze such complicated interaction problems.

Calabrese and Monaco (2001) studied the stresses induced in existing deep tunnels (storing liquefied gas) by pile driving from the ground surface. A 2D plane strain analysis (Finite Difference Method) was carried out using FLAC. Then, dynamic analysis of pile driving was performed. In all the calculation stages, the soil behavior was described by the Mohr-Coulomb model. It is of importance to note that non-linear soil behavior, (i.e., shear modulus G decreases with shear strain γ_{xy} , also see Cheng *et al.* 2002) was adopted in the soil layer containing the tunnel during simulation of excavation. The results of the analysis indicated that the increase in stresses in the lining was moderate and below the admissible stress level of concrete.

Many researchers studied this interaction. Some of them focused on numerical simulations (e.g., Mroueh and Shahrour 2003, Surjadinata *et al.* 2006, Huang *et al.* 2009) where their analyses were based on the tunnel pile interaction and they applied various constitutive models of the soil. In addition they studied the geometry effect and whether the foundation is single pile or grouped piles in 2D or 3D. Other researchers used the experimental methods in studying the behavior of piles due to tunneling (Lee and Bassett 2007, Meguid and Mattar 2009) to investigate many factors which may limit the effects of tunnel excavation processes on nearby piles, and to provide realistic results for verification against numerical methods results. Most of these studies were conducted in the laboratory by using specific techniques (e.g., photo-elasticity technique, photogrammetric technique, small scale testing model, etc.). Abdullah and Taha (2013) summarized the selected studies dealing with the effects of tunneling on nearby piles, including numerical methods and laboratory model tests.

Laboratory model investigations of piles behavior remain popular because of the high cost of field testing and the better possibility of achieving specific soil characteristics in a laboratory environment. The monitored behavior of model structures has led to a better understanding of pile foundations and enables more reliable and economical design to be employed (Chore and Siddiqui 2013, Fattah *et al.* 2015).

The main purpose of the experimental research implemented in this work is to study the interaction effect between pile groups and tunnels constructed underneath. The load sharing mechanism between piles and the raft besides the load-settlement behavior will be considered. The test setup used to perform the model tests, the mechanical properties of the investigated soil, the configuration of prototype pile groups and piled rafts, the measurements performed and the testing program and procedure will be described.

2. Experimental study

All model tests were conducted using the setup shown in Fig. 1, which consists of a soil tank, model pile groups, tunnels, and a loading frame. The vertical load was applied on the model piles

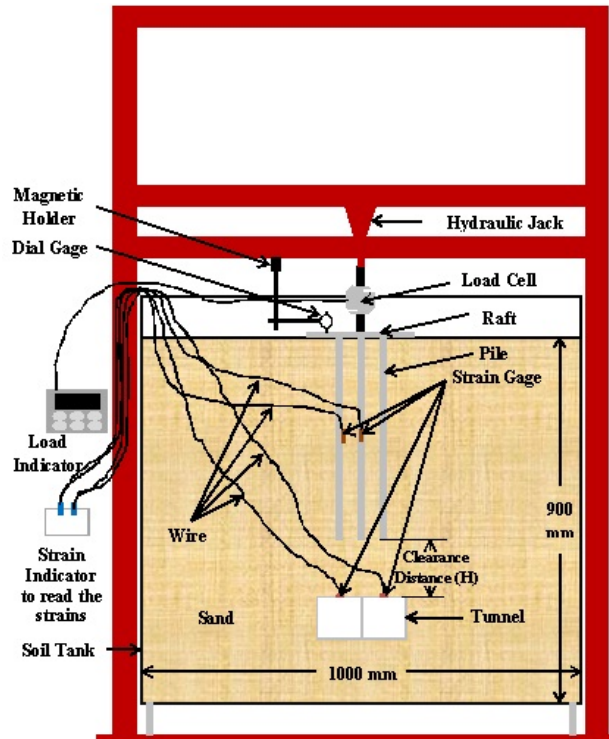


Fig. 1 Setup of the laboratory model

by means of a hydraulic jack 2 tons capacity. The applied load was measured using a load cell of 2 tons capacity. A dial gauge with 0.01 mm sensitivity was used for measuring settlements at the centerline of the piled raft model. Strain gages, 6 mm long, were adhered to piles and tunnels and connected to a strain indicator to measure the strains in piles and tunnels.

The soil tank dimensions are 1 m length, 1 m width, and 1 m height resting on a steel rail stiffened by 2 lines of 50 mm steel angles with thickness of 4 mm. The tank is provided with 3 sides of plywood of, 1.1 m × 1 m, which can slide for sand unloading and 1 side made of glass in the front of the soil tank. The dimensions of the tank were chosen so that there will be no interference between the walls of the soil tank and the pile groups and tunnels system. Furthermore, the internal sides of the tank are made of smooth plywood in order to minimize friction, if any, that may develop between the steel tank surfaces and the soil and to minimize the weight of soil tank.

2.1 Soil properties

The soil used for the model tests is clean, oven-dried, uniform quartz sand obtained from Kerbela governorate 100 km south west of Baghdad. The tests are performed on medium dense sand, the maximum and minimum dry unit weights of sand were determined according to the ASTM (D4253-2000) and ASTM (D4254-2000) specifications, respectively. The specific gravity test is performed according to ASTM (D854-2005) and the grain size distribution is analyzed according to ASTM (D422-2001) specifications. Table 1 shows the physical properties of the tested sand.

Table 1 Physical properties of the tested sand

Property	Value
The angle of internal friction, ϕ	37°
Grain size analysis	
Effective size, D_{10}	0.23 mm
Coefficient of uniformity, C_u	3.913
Coefficient of curvature, C_c	0.893
Classification (USCS)*	SP
Specific gravity, G_s	2.66
Dry unit weights	
Maximum dry unit weight, $\gamma_{d(\max)}$	17.22 kN/m ³
Minimum dry unit weight, $\gamma_{d(\min)}$	14.10 kN/m ³
Test dry unit weight, $\gamma_{d(\text{test})}$	15.92 kN/m ³
Relative density, D_r	63%
Void ratio	
Maximum void ratio, e_{\max}	0.85
Minimum void ratio, e_{\min}	0.52
Test void ratio, e_{test}	0.64
Porosity	
Maximum porosity, n_{\max}	0.46
Minimum porosity, n_{\min}	0.34
Test porosity, n_{test}	0.39

* USCS refers to Unified Soil Classification System

Table 2 Mechanical properties of the used aluminum alloy

Property	Value
Minimum yield strength (N/mm ²)	275
Minimum ultimate yield strength (N/mm ²)	310
Minimum % of elongation	12
Modulus of elasticity (N/mm ²)	70000
Poisson's ratio	0.33

2.2 Piles, raft and tunnels models

The piles used in this study are modeled using smooth aluminum hollow section having square cross sections of 25 mm × 25 mm and thicknesses of 1.5 mm. The embedment (depth to width) ratio L/d is equal to 8, 14 and 20 where L represents the pile length and d is the outside width of the pile. The spacing between piles is kept constant at $3d$ ($s = 75$ mm, where s is the spacing between piles) in all tests.

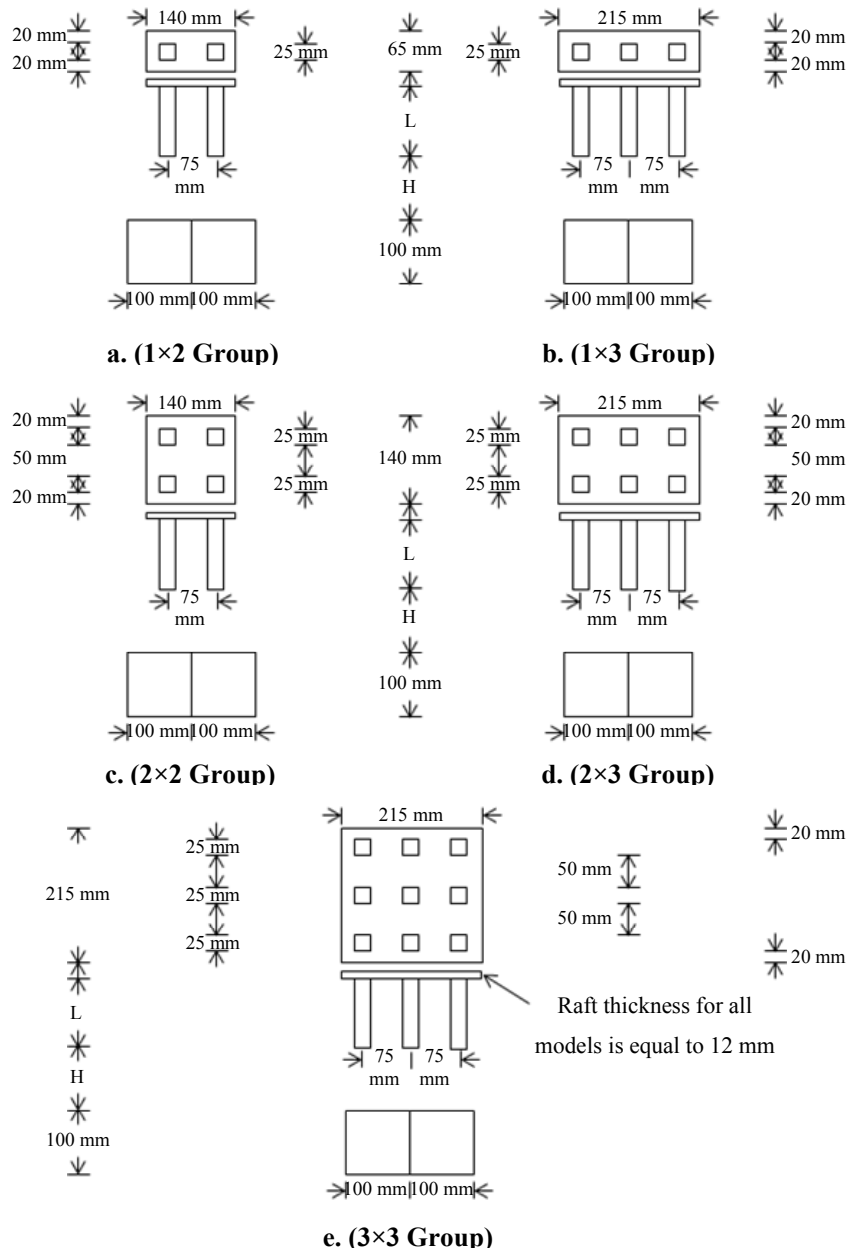


Fig. 2 Pile group configurations adopted in the experimental tests

The raft used in the test was also modeled using aluminum with smooth surface and thickness of 12 mm (two plates each one has thickness of 6 mm are connected together by bolts and nuts).

The tunnels are modeled using smooth aluminum hollow section having a square cross section of 100 × 100 mm and a thickness of 2 mm. Piles, raft and tunnels were composed of ALUPCO alloy, which is supplied locally by ALUPCO Alloys Company, according to the technical specification and mechanical properties shown in Table 2.

2.3 Testing program

A program for performing a parametric study on tunnels underlying pile group models was carried out by testing five pile configurations with different pile lengths of (200 mm), (350 mm) and (500 mm), width (25 mm), spacing (75 mm). The same raft thickness (12 mm) and tunnel outside width (100 mm), thickness (2 mm) and length (1000 mm) are used. The testing program is shown in Fig. 2.

2.4 Load carrying capacity of pile groups

This section presents the load carrying capacity of piles in each group as well as the load settlement behavior of the whole system. The tangent method is used in this study for determination of ultimate bearing capacity and working load from the load-settlement relations of pile groups for all models. Each pile has constant cross sectional area, outside width (d) of 25 mm (square cross section) and different lengths (L) of 200, 350 and 500 mm. The raft thickness ($t_r = 12$ mm) and the spacing between piles ($s = 75$ mm) are kept constant. In the following figures, the settlement at mid-point is plotted against the vertical applied load at center.

Fig. 3 shows the load settlement behavior of piled raft - tunnel interaction for the group of (1×2) with different pile lengths ($L = 200, 350$ and 500 mm). The distance between pile tip and the top surface of tunnel (clearance distance) is $H = 130$ mm and the least width containing pile group is

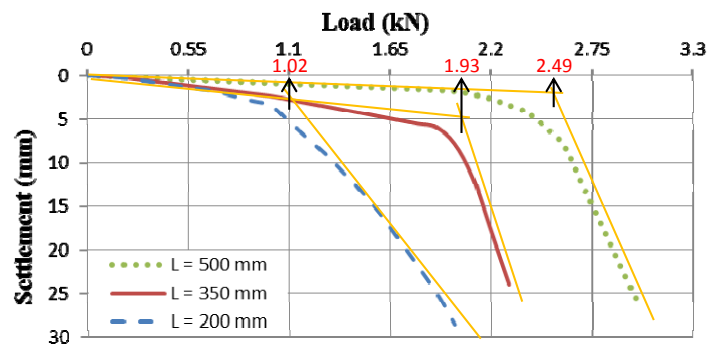


Fig. 3 Load – settlement curve for (1×2) piled raft-tunnel, ($H = 130$ mm) and ($B/H = 0.192$)

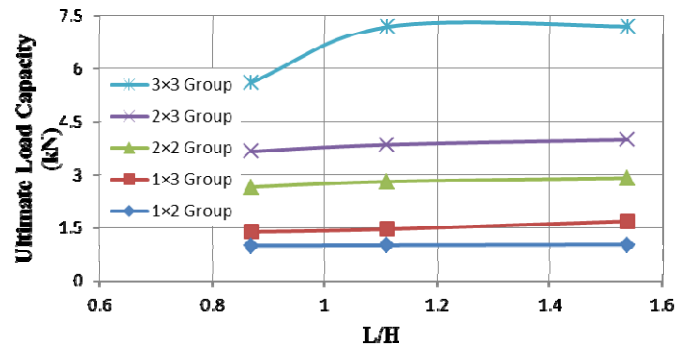


Fig. 4 Ultimate load capacity of group versus (L/H) for all pile groups with ($L = 200$ mm) and ($H = 130, 180$ and 230 mm)

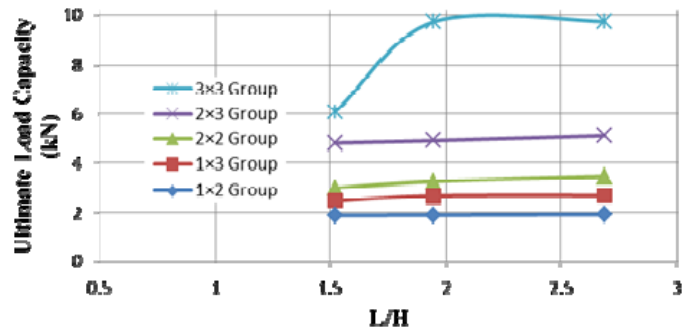


Fig. 5 Ultimate load capacity of group versus (L/H) for all pile groups with ($L = 350$ mm) and ($H = 130, 180$ and 230 mm).

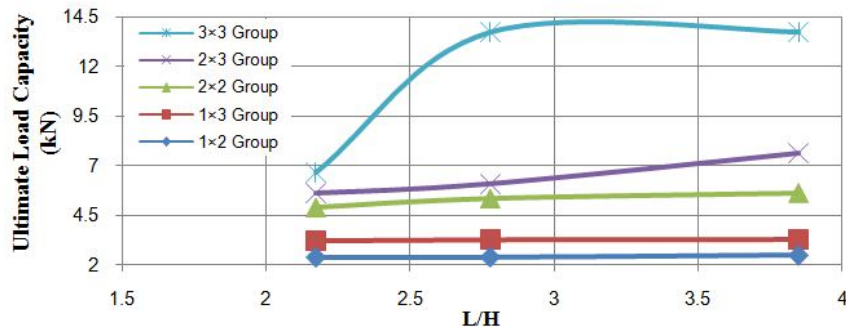


Fig. 6 Ultimate load capacity of group versus (L/H) for all pile groups with ($L = 500$ mm) and ($H = 130, 180$ and 230 mm)

$B = 25$ mm. The ratio (B/H) is equal to 0.192 for this case. From this figure, the load carrying capacity increases with increasing the length of piles.

The Figs. 4, 5 and 6 show the effect of the (L/H) ratio on ultimate load capacity for different pile groups. It is obvious that increasing pile length will cause an increase in the ultimate load for different pile configuration. Also, it is obvious that increasing the distance between pile tips and the top surface of the tunnel will cause a decrease in the ultimate load and that the effect of (L/H) ratio on ultimate load will be larger for 3×3 pile group and lesser for other groups. According to Figures, the increase of number of piles to 3×3 implies a significant increase in the dimensional size of the group. This will cause a significant increase in the size of the stress bulb and hence the ultimate load particularly when expressed as a force (kN).

2.5 Load carrying capacity of piles in the group and piles share

The total load carried only by piles can be obtained by knowing the load in each individual pile. The pile group model is placed at a vertical distance ≥ 5 mm above top surface of sand as shown in Fig. 7. The strain in a pile is obtained when the reading of strain indicator becomes constant with the increase of settlement as shown in Fig. 8. The load in that pile can be calculated if the cross sectional area and the modulus of elasticity of piles are known (pile total load = modulus of elasticity \times strain \times area).

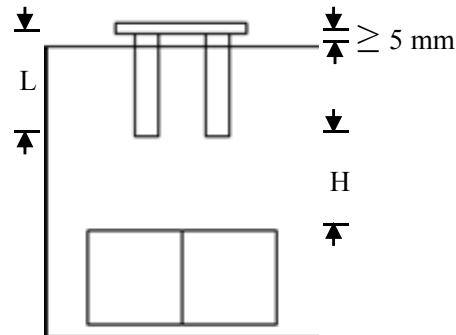
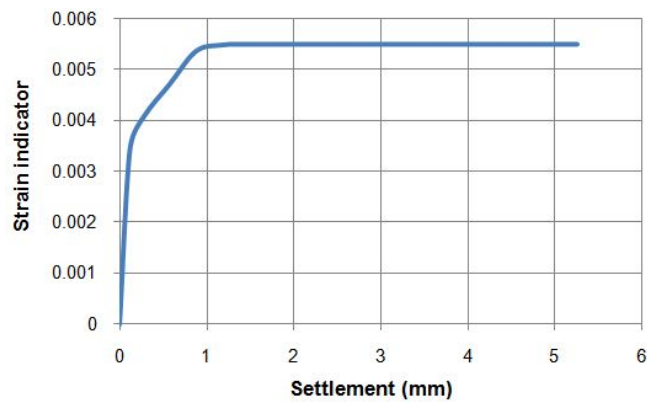
Fig. 7 Vertical distance of raft base ≥ 5 mm above top surface of sandFig. 8 Strain indicator versus settlement for the group of (1×2) piles with pile length (L) of 200 mm and clearance distance (H) of 130 mm

Table 3 Piles capacity for the studied cases

Group		Piles capacity (N)			Piles share (%)
		$H = 130$ mm	$H = 180$ mm	$H = 230$ mm	
(1×2) Group,	$L = 200$ mm	400	389	389	39
	$L = 350$ mm	791	782	782	41
	$L = 500$ mm	1140	1100	1092	46
(1×3) Group,	$L = 200$ mm	763	657	624	45
	$L = 350$ mm	1297	1292	1193	48
	$L = 500$ mm	2047	2035	2004	62
(2×2) Group,	$L = 200$ mm	1366	1322	1257	47
	$L = 350$ mm	1994	1877	1730	57
	$L = 500$ mm	4419	4190	3793	78
(2×3) Group,	$L = 200$ mm	2801	2693	2558	70
	$L = 350$ mm	3650	3513	3440	72
	$L = 500$ mm	6304	5037	4608	82

Table 3 Continued

Group	Piles capacity (N)			Piles share (%)	
	$H = 130$ mm	$H = 180$ mm	$H = 230$ mm		
(3×3) Group,	$L = 200$ mm	6396	6396	5001	89
	$L = 350$ mm	8718	8718	5498	90
	$L = 500$ mm	12640	12627	6153	92

The total load carried only by piles can be obtained by knowing the load in each individual pile. The total carrying capacity of the piles relative to the total applied load (the piles share) increases also with increasing pile length, number of piles in the group and the ratio (B/H). The group of (3×3) with ($L = 500$ mm and $B/H = 1.346$) recorded the maximum piles capacity with 92% of the total applied load. The pile share was not affected by the value of (H) for the same pile length and number of piles in the group. The piles carrying capacity and piles share for the studied groups with different lengths and H values are given in Table 3.

The load capacity of the piles in the piled raft-tunnel system (pile sharing) is affected directly and sometimes slightly by (L/H) ratio. Figs. 9, 10 and 11 show the effect of (L/H) ratio for all groups on pile sharing. From these figures, the piles share increases with increasing (L/H) ratio and increasing number of piles in the group. This is due to the increase of skin resistance of the pile which leads to increase in pile contribution to the bearing capacity.

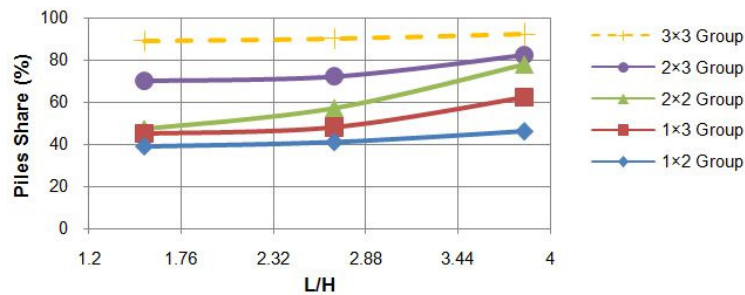


Fig. 9 Effect of the ratio (L/H) on the piles share for all pile groups with ($L = 200, 350$ and 500 mm) and ($H = 130$ mm)

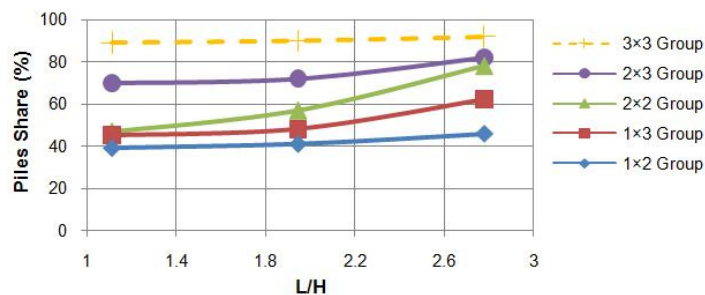


Fig. 10 Effect of the ratio (L/H) on the piles shared for all pile groups with ($L = 200, 350$ and 500 mm) and ($H = 180$ mm).

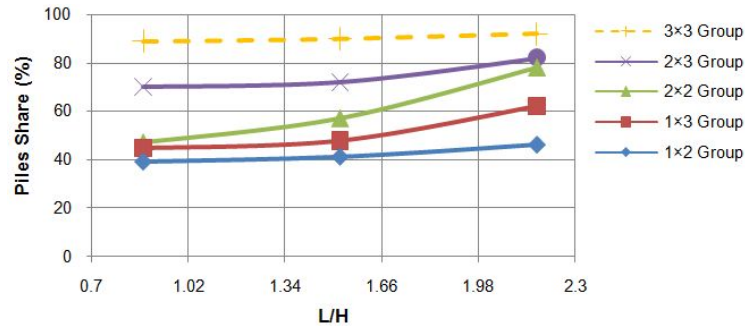


Fig. 11 Effect of the ratio (L/H) on the piles shared for all pile groups with ($L = 200, 350$ and 500 mm) and ($H = 230$ mm).

3. Finite element analysis

In the present study, three-dimensional 8-node solid elements are used to model the piled raft and soil. The elements have eight corner nodes, and each node has three degrees of freedom. In the finite element solution, both the soil and piled raft-tunnel systems are meshed with the 8-node brick solid 45 elements. In the ANSYS computer program, the interaction is simulated through defining surfaces with volume glue (as the case of pile-soil interaction and raft-soil interaction). The piled raft-tunnel model is assumed to be linearly elastic material having the following assumed properties:

Young modulus $E_a = 70 \times 10^6$ kN/m² and
Poisson's ratio $\nu_a = 0.33$

The soil is modeled as elasto-plastic material according to the Drucker-Prager constitutive relation. The soil measured parameters used in the Drucker-Prager constitutive model are:

Young modulus $E_s = 50 \times 10^3$ kN/m²,
Poisson's ratio $\nu_s = 0.35$,
Cohesion $c_u = 0.3$ kN/m² and
Angle of internal friction (ϕ) = 37°

Fig. 12 shows the numerical load settlement behavior of piled raft-tunnel interaction for the pile group (1x2) with different pile lengths ($L = 200, 350$ and 500 mm). From this figure, the load carrying capacity increased with increasing pile lengths due to the fact that the soil becomes stiffer with depth and due to the increase in skin friction of piles.

Also, in Fig. 12, the same conclusion is obtained from experimental load settlement behavior of piled raft-tunnel interaction except that there is a slight difference between the total load capacity and maximum settlement of the experimental and numerical results. The obtained experimental values are greater than that obtained from finite elements.

The maximum difference between the experimental total load capacity and the numerical was 2.58 kN (17%) in case of (3x3) group with ($L = 500$ mm and $H = 180$ mm). The maximum difference between the maximum settlement (the settlement of center of the raft surface) of the experimental and that of the numerical was 3.229 mm (10.7%) in case of (2x2) group with ($L = 350$ mm and $H = 230$ mm).

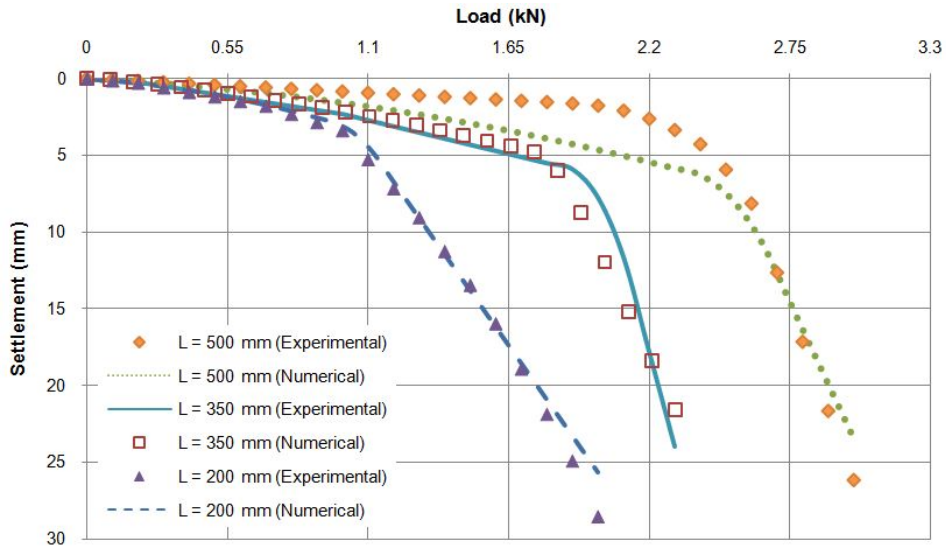


Fig. 12 Experimental and Numerical load – settlement curves for (1×2) piled raft-tunnel ($H = 130$ mm) and ($B/H = 0.192$).

3.1 Parametric study

The behavior of piled raft-tunnel system can be influenced by several factors such as the arrangement of piles, length of pile (L), the distance between pile tips and top surface of tunnel (clearance distance) (H) and other factors.

In this section, the effect of raft thickness, the tunnel thickness, the tunnel width and the angle of inclination of the applied load (applied at center of the raft) on the performance of maximum von Mises stress and settlement of piled raft-tunnels of the (1×2) pile group with length of 200 mm and clearance distance of 130 mm are studied.

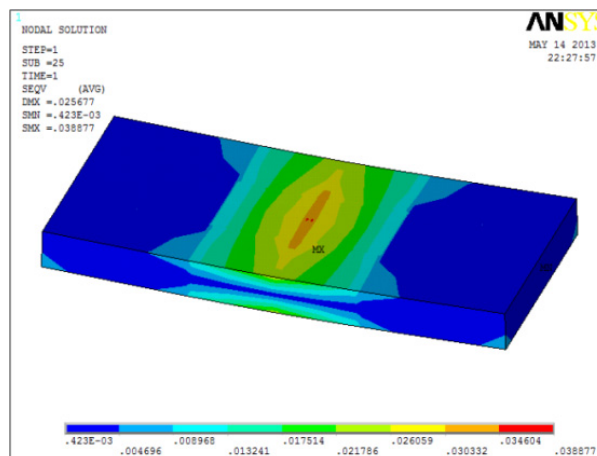


Fig. 13 Variation of von Mises stress for (1×2) pile group with $L = 200$ mm, $H = 130$ mm and $t_r = 12$ mm

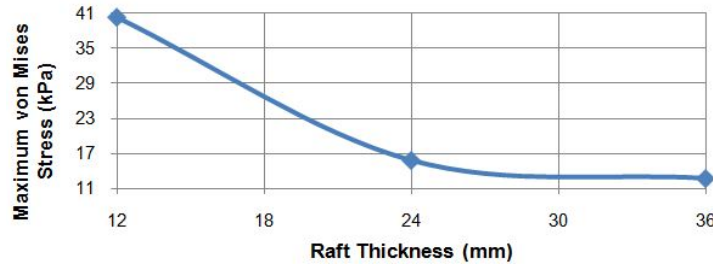


Fig. 14 Raft thickness versus the maximum von Mises stress of piled raft-tunnels for the group of (1×2) with ($L = 200$ mm) and ($H = 130$ mm)



Fig. 15 Raft thickness versus the maximum settlement of piled raft-tunnels for the group of (1×2) with ($L = 200$ mm) and ($H = 130$ mm).

3.1.1 Effect of raft thickness (t_r)

The effect of raft thickness on the maximum von Mises stress and settlement (at the center of the raft) of piled raft-tunnels was studied with three different thicknesses (12, 24 and 36 mm) as shown in Fig. 13.

Fig. 14 shows the maximum von Mises stress plotted against raft thickness while in Fig. 15 the maximum settlement is plotted against raft thickness. It can be seen that maximum von Mises stress and maximum settlement were decreased by 70% and 15%, respectively with increasing raft thickness from 12 mm to 36 mm at the same magnitude of applied load because of increasing raft stiffness.

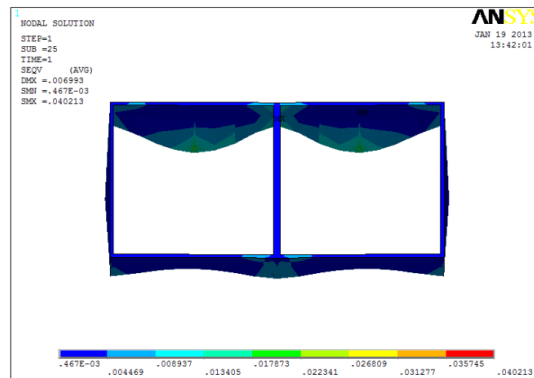


Fig. 16 Variation of von Mises stress for (1×2) pile group with $L = 200$ mm, $H = 130$ mm and $t_r = 2$ mm

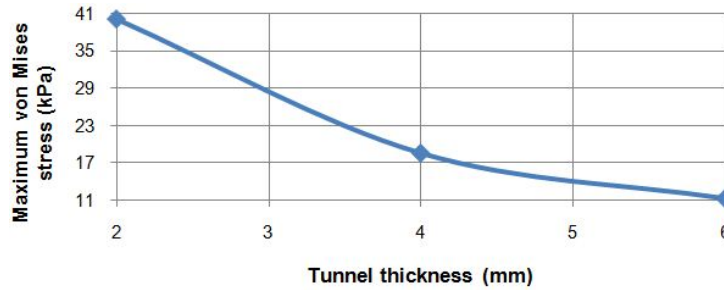


Fig. 17 Tunnel thickness versus the maximum von Mises stress of piled raft-tunnels for the group of (1×2) with ($L = 200$ mm) and ($H = 130$ mm)

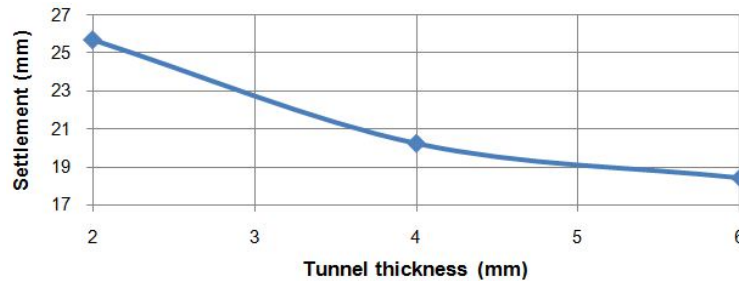


Fig. 18 Tunnel thickness versus the maximum settlement of piled raft-tunnels for the group of (1×2) with ($L = 200$ mm) and ($H = 130$ mm)

3.2 Effect of tunnel thickness (t_t)

The effect of the tunnel thickness on the maximum von Mises stress and settlement of piled raft-tunnels was studied with three different thicknesses (2, 4 and 6 mm) as shown in Fig. 16.

Fig. 17 shows the maximum von Mises stress plotted against tunnel thickness while in Fig. 18, the maximum settlement is plotted against tunnel thickness. It can be seen that maximum von Mises stress and maximum settlement is decreased by 70% and 28% respectively with increasing tunnel thickness from 2 mm to 6 mm at the same magnitude of applied load because of increasing the tunnel stiffness.

3.3 Effect of tunnel width (w_t)

The effect of the tunnel width on the maximum von Mises stress and settlement of piled raft-tunnels was studied using three different widths (100, 200 and 300 mm). Fig. 19 shows the maximum von Mises stress plotted against tunnel width while in Fig. 20, the maximum settlement is plotted against tunnel width. It can be seen that maximum von Mises stress and maximum settlement were decreased by 87% and 9%, respectively with increasing tunnel width from 100 mm to 300 mm at the same magnitude of applied load because of increasing tunnel stiffness.

3.4 Effect of the angle of inclination of the applied force (θ)

The effect of the angle of inclination, from the horizontal axis, of the applied load on the maximum von Mises stress, horizontal and vertical displacements of piled raft-tunnels is studied

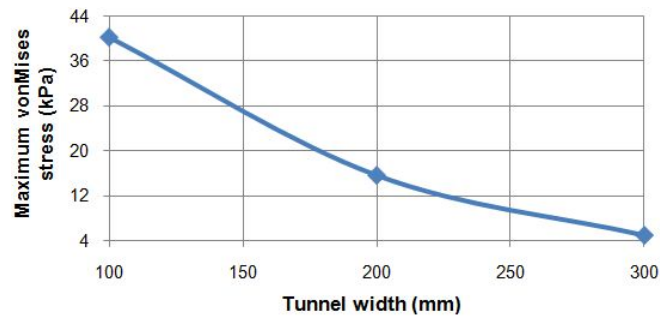


Fig. 19 Tunnel width versus the maximum von Mises stress of piled raft-tunnels for the group of (1×2) with ($L = 200$ mm) and ($H = 130$ mm).

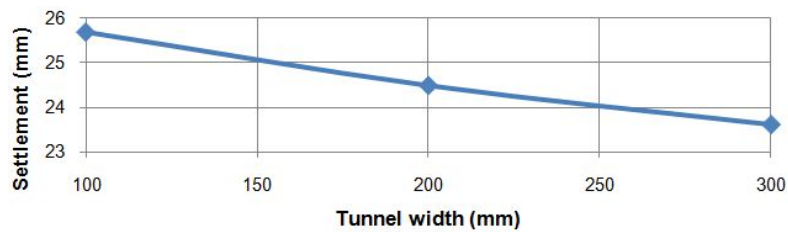


Fig. 20 Tunnel width versus the maximum settlement of piled raft-tunnels for the group of (1×2) with ($L = 200$ mm) and ($H = 130$ mm)

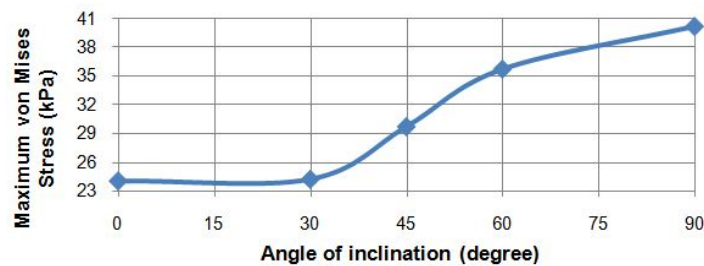


Fig. 21 Angle of inclination of the applied load versus the maximum von Mises stress of piled raft-tunnels for the group of (1×2) with ($L = 200$ mm) and ($H = 130$ mm)

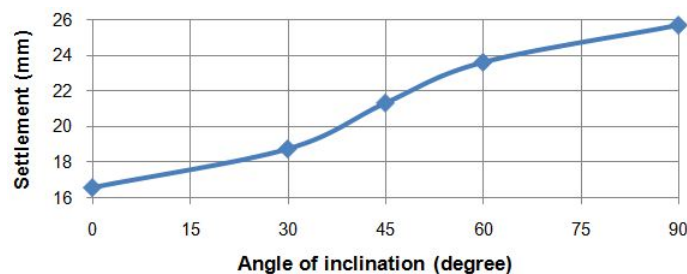


Fig. 22 Angle of inclination of the applied load versus the maximum vertical settlement of piled raft-tunnels for the group of (1×2) with ($L = 200$ mm) and ($H = 130$ mm)

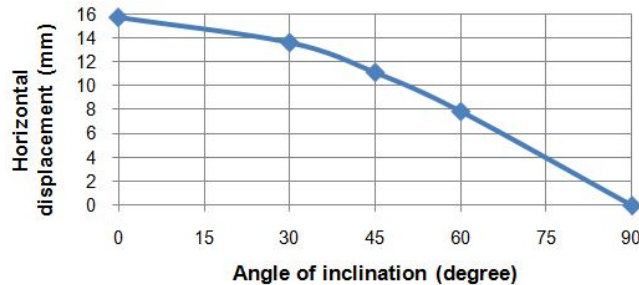


Fig. 23 Angle of inclination of the applied load versus the maximum horizontal displacement of piled raft-tunnels for the group of (1×2) with ($L = 200$ mm) and ($H = 130$ mm)

using five angles with respect to the horizontal axis (0, 30, 45, 60 and 90°). Fig. 21 shows the maximum von Mises stress plotted against angle of inclination of the applied load whereas Fig. 22 shows the maximum vertical settlement plotted against angle of inclination of the applied load. Fig. 23 shows the maximum horizontal displacement plotted against angle of inclination of the applied load. It can be seen that maximum von Mises stress and maximum vertical settlement were increased by 40% and 35%, respectively and horizontal displacement was decreased by 100% with increasing angle of inclination of the applied load from 0 to 90°.

4. Conclusions

The experimental and finite elements modeling implemented in the present study yield the following major conclusions:

- The load carrying capacity of the piled raft-tunnel model increased by about 93% with increasing pile lengths by 250% for variable (H) distance.
- The total carrying capacity of the piled raft-tunnel model decreased by a percentage ranging from 3% for (1×2) group to 50% for (3×3) group with increasing the distance between pile tips and the top surface of the tunnel (H) by 177% for constant pile lengths.
- The total load carrying capacity of the piled raft-tunnel model decreases with decreasing number of piles in the group. The percentage decrease in ultimate loads with reference to the (3×3) group are about 90%, 81%, 65% and 47% for (1×2), (1×3), (2×2) and (2×3) respectively and for variable pile lengths and variable distance between pile tips and the top surface of the tunnel.
- The total load carrying capacity of the piles relative to the total applied load (piles share) increases with increasing pile lengths, the number of piles in the group and the (B/H) ratio. The group of (3×3) with ($L = 500$ mm and $B/H = 1.346$) recorded the maximum piles capacity with 92% of the total applied load. But it was not affected by the value of (H) for the same pile length and number of piles in the group.
- The increase in pile length to clearance distance between pile tips to the top surface of the tunnel ratio (L/H) for variable (H) distance leads to an increase in piles share by 15%, 27%, 40% , 15% and 3% for the (1×2), (1×3), (2×2), (2×3) and (3×3) groups respectively. Also, piles share increased by 50% with increasing the number of piles in the group from (1×2) to (3×3) for pile length of 500 mm. This is due to the increase in the bearing capacity of piles

as a result of increasing the skin resistance of each pile.

- The maximum von Mises stress and maximum settlement were decreased by 70% and 15%, respectively, with increasing raft thickness from 12 mm to 36 mm at the same magnitude of applied load.
- The maximum von Mises stress and maximum settlement were decreased by 70% and 28%, respectively, with increasing tunnel thickness from 2 mm to 6 mm at the same magnitude of applied load.
- The maximum von Mises stress and maximum settlement were decreased by 87% and 9%, respectively, with increasing tunnel width from 100 mm to 300 mm at the same magnitude of applied load.
- The maximum von Mises stress and maximum settlement were increased by 40% and 35%, respectively, and horizontal displacement decreased by 100% with increasing angle of inclination of the applied load from 0 to 90° from the horizontal axis.

References

- Abdullah, M.H. and Taha, M.R. (2013), "A review of the effects of tunneling on adjacent piles", *Electric. J. Geotech. Eng.*, **18**, 2739-2762.
- ANSYS 12.1 (2010), ANSYS 12.1 Finite element analysis system help, SAS IP, Inc.
- ASTM D422-2001 (2001), Standard test method for particle size-analysis of soils.
- ASTM D4253-2000 (2000), Standard test method for maximum index density and unit weight of soils using a vibratory table.
- ASTM D4254-2000 (2000), Standard test method for minimum index density and unit weight of soils and calculation of relative density.
- ASTM D854-2005 (2005), Standard test method for specific gravity of soil solids by water pycnometer.
- Benton, L.J. and Phillips, A. (1991), "The behavior of two tunnels beneath a building on piled foundations", *Proceedings of the 10th European Conference on Soil Mechanics and Foundation Engineering*, Florence, Italy, May, pp. 665-668.
- Calabrese, M. and Monaco, P. (2001), "Analysis of stresses induced in an old deep tunnel by pile driving from the surface", *Proceedings of the 2nd FLAC Symposium on Numerical Modeling in Geomechanics*, Lyon, France, October, pp. 199-204.
- Cheng, C.Y., Dasari, G.R., Leung, C.F. and Chow, Y.K. (2002), "A novel FE technique to predict tunneling induced ground movement in clays", *Proceedings of the 15th KKCNN Symposium on Civil Engineering*, Singapore, October, pp. 43-48.
- Chore, H.S. and Siddiqui, M.J. (2013), "Analysis of the piled raft for three load patterns: A parametric study", *Coupled Syst. Mech., Int. J.*, **2**(3), 289-302.
- Cox, W.R., Dixon, D.A. and Murphy, B.S. (1984), "Lateral-load tests on 25.4-mm (1-in.) diameter piles in very soft clay in side-by-side and in-line groups, laterally loaded deep foundations: Analysis and performance", ASTM STP 835, pp. 122-139.
- Fattah, M.Y., Yousif, M.A. and Al-Tameemi, S.M.K. (2015), "Effect of pile group geometry on bearing capacity of piled raft foundations", *Struct. Eng. Mech., Int. J.*, **54**(5), 829-853.
- Huang, M., Zhang, C. and Li, Z. (2009), "A simplified analysis method for the influence of tunneling on grouped piles", *Tunn. Undergr. Space Technol.*, **24**(4), 410-422.
- Lee, Y.J. and Bassett, R.H. (2007), "Influence zones for 2D pile-soil-tunneling interaction based on model test and numerical analysis", *Tunn. Undergr. Space Technol.*, **22**(3), 325-342.
- Meguid, M.A. and Mattar, J. (2009), "Investigation of tunnel-soil-pile interaction in cohesive soils", *J. Geotech. Geoenviron. Eng., ASCE*, **135**(7), 973-979.
- Mokwa, R.L. (1999), "Investigation of the resistance of pile caps to lateral loading", Ph.D. Dissertations;

Virginia Polytechnic Institute and State University, Blacksburg, VA, USA.

Mroueh, H. and Shahrour, I. (2003), "A full 3-D finite element analysis of tunneling-adjacent structures interaction", *Comput. Geotech.*, **30**(3), 245-253.

Surjadinata, J., Hull, T.S., Carter, J.P. and Poulos, H.G. (2006), "Combined finite- and boundary-element analysis of the effects of tunneling on single piles", *Int. J. Geomech.*, **6**(5), 374-377.

CC